Ferromagnetic resonance studies in granular Co – Si O 2 thin films

M. J. M. Pires, J. C. Denardin, E. C. da Silva, and M. Knobel

Citation: Journal of Applied Physics **99**, 063908 (2006); doi: 10.1063/1.2186382
View online: http://dx.doi.org/10.1063/1.2186382
View Table of Contents: http://scitation.aip.org/content/aip/journal/jap/99/6?ver=pdfcov
Published by the AIP Publishing

Ferromagnetic resonance studies in granular Co–SiO_2 thin films

M. J. M. Pires, J. C. Denardin,[a] E. C. da Silva, and M. Knobel
Instituto de Física Gleb Wataghin, Universidade Estadual de Campinas, Unicamp, Caixa Postale 6165, 13083-970, Campinas, São Paulo, Brazil

(Received 7 June 2005; accepted 14 February 2006; published online 29 March 2006)

Properties of thin granular Co–SiO_2 films have been studied by means of ferromagnetic resonance (FMR). The obtained FMR results are discussed using sample magnetization, electrical conductivity, and transmission electron microscopy analysis. Co and SiO_2 were sequentially deposited for the sample preparation. The general behavior of the applied field for resonance could be described using effective out-of-plane anisotropies. A dipolar interaction model developed for magnetic heterostructures was applied to the interpretation of these anisotropies. The anisotropy terms caused by the magnetic particle shapes and by the film shape can explain the results for two metallic films close to percolation, in which the film shape is the preponderant contribution. In the case of an insulating sample, the consideration of an additional anisotropy term seems to be necessary to explain the results. © *2006 American Institute of Physics*. [DOI: 10.1063/1.2186382]

I. INTRODUCTION

The development of a detailed understanding of the effects of interparticle interactions represents one of the most important tasks of the renewed interest in magnetic nanoparticles. The problem is extremely complex because these granular systems have a very rich variety of magnetic configurations, resulting from different shapes, dispersions, and sizes of magnetic clusters. The interparticle interaction (exchange and/or dipolar) competes with the magnetic anisotropy in determining the orientation of the particle moments. Ferromagnetic resonance (FMR) is a complementary technique to study these phenomena. It is particularly sensitive to medium heterogeneity variations and to the anisotropies in question. Contributions to the magnetic behavior related to distinct magnetic structures of the medium can also be identified by FMR. The high sensitivity of this technique has been widely employed in the investigation of magnetic interaction in nanostructured magnetic systems in general.[1–5] For real samples, the number of structural configurations contributing to the magnetic behavior is too large to carry out general calculations, and therefore, several simplifications have been used. The use of a mean isotropic exchange coupling reaching the whole sample, assuming bulk values for the actual exchange stiffness constant, is one example of such a simplification.[1,2,4] It is also very common in systems with metallic matrix to treat of the coupling between magnetic layers as a Ruderman-Kittel-Kasuya-Yosida (RKKY) -like interaction.[6] Another example is assuming the continuity of the magnetization in the calculation of the magnetic self-energy, which is a linear combination of the limiting cases of isolated particles and a homogeneously magnetized sample.[7]

In order to best understand the interplay between dipolar interaction and anisotropies on the magnetic properties of nanostructured systems, thin Co–SiO_2 films with different nanostructures were studied by means of FMR. The studied films were produced by sequential deposition. This kind of deposition allows a better control of the sizes and distances among the magnetic clusters, differently from codeposition methods, which usually result in a large dispersion of particle size and interparticle distances.

The obtained FMR results are discussed together with sample magnetization, electrical conductivity, and transmission electron microscopy (TEM) analysis. Samples with different electrical conductance and magnetic behavior are compared. For the interpretation of the observed anisotropies, we have applied a dipolar interaction model developed for magnetic heterostructures.[7] This interpretation allows for a general discussion regarding the magnetic interactions between the magnetic clusters.

II. EXPERIMENTAL

Co/SiO_2 multilayers were grown by dc (Co) and rf (SiO_2) sputtering on Si substrates held at room temperature. A 10 nm buffer layer of SiO_2 was deposited on the Si substrate before the sequential deposition. By varying the nominal thickness of Co and SiO_2 layers, we obtained different samples, ranging from insulating to metallic. The samples here studied are labeled as (1) Co(0.7 nm)/SiO_2(1.8 nm); (2) Co(0.8 nm)/SiO_2(2 nm), and (3) Co(1 nm)/SiO_2(2 nm). The above thicknesses are the nominal values based on the preparation equipment calibration and would be the expected final thicknesses of the layers if the materials were uniformly and continuously deposited on the substrates. The samples are a result of a sequential deposition of 10 bilayers each.[10]

In the FMR measurements, pieces of about 3×3 mm^2 of the samples were used. A Varian E-12 spectrometer operating at *x* band (9.54 GHz) and room temperature has been employed. Cross-section TEM characterization was performed using a Jeol JEM-3010 angle-resolved photoemission (ARP) microscope. Magnetization and transport properties were measured in the Quantum Design MPMS XL7 system in the temperature range 5–300 K and fields up to 20 kOe.

[a]Present address: Departamento de Física, Universidad de Santiago de Chile, USACH, Santiago, Chile.

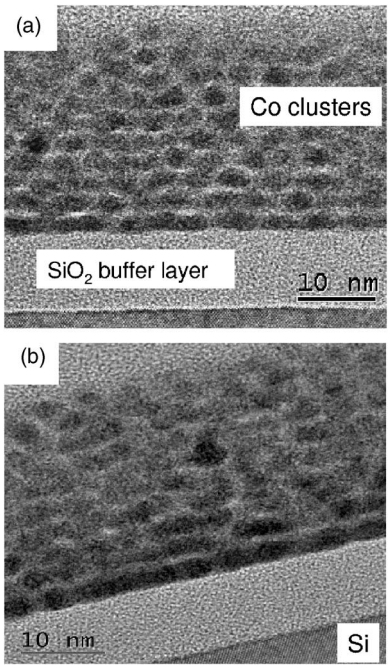

FIG. 1. Cross-section TEM images of (a) the granular multilayer 1 and (b) the percolated multilayer 3.

III. RESULTS AND DISCUSSION

A. Characterization of the samples

Cross-section TEM images of samples 1 and 3 are shown in Fig. 1. Sample 1 has slightly flattened Co grains of about 3 nm in diameter, which are well defined and separated from each other [Fig. 1(a)]; while in sample 3, the Co grains touch each other forming irregular Co layers, as can be seen in Fig. 1(b). From an analysis of previous magnetic and conductivity results, we can infer that the structure of sample 2 is closer to that of sample 3 than of sample 1.

The resistivity curve as a function of temperature for sample 1 could be well fitted by a $\log(\rho)=\rho_o \exp[(T_o/T)^{1/2}]$ law, which is typical of insulating granular systems and can be attributed to thermally activated and/or bias assisted tunneling processes.[8] Sample 2 behaves as a typical metal with impurities ($\rho=a+bT$), and sample 3 shows a $-\log(T)$ dependence which can be attributed to weak localization or electron-electron interaction effects in a disordered metallic system.[8,9]

The magnetization curves, measured at room temperature, are predominantly ferromagnetic (FM) for samples 2 and 3 and mainly superparamagnetic (SPM) for sample 1. The hysteresis in the $M(H)$ magnetization loops is smaller than 50 Oe for all samples. The general form of the magnetization can be interpreted as the sum of a constant and a Langevin curve, where the former term is due to blocked magnetic grains and the Langevin term is due to small grains which are SPM at room temperature.

B. FMR measurements

As the magnetizations of the samples are not saturated at the resonance fields, mainly for the parallel configuration, the FMR spectral parameters have been obtained from fits with the expression $y=-M(H)2A\Gamma^2(H-H_{res})/[\Gamma^2+(H-H_{res})^2]^2$, where M is the magnetization, A is a scale factor, H the applied magnetic field, H_{res} the resonance field, and Γ the half-width at half-height. The term that follows $M(H)$ is the first derivative of a Lorentzian curve with respect to the applied field. When two resonance lines were detected, an additional such derivative was included in y. The $M(H)$ curve for each sample was obtained also fitting the experimental curves, using a Langevin curve plus a constant. An example of this procedure is presented in Fig. 2.

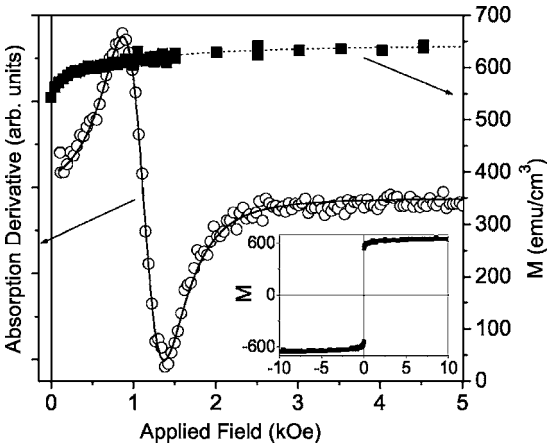

FIG. 2. Example of spectral fit used for obtaining the FMR parameters. Sample 3, at parallel configuration and room temperature. The experimental $M(H)$ curve (full squares) is fitted with a Langevin curve plus a constant (dotted line). Such a $M(H)$ curve is then used in $y=-M(H)2A\Gamma^2(H-H_{res})/[\Gamma^2+(H-H_{res})^2]^2$, in order to fit (solid line) the FMR spectra (open circles). The inset shows the complete magnetization loop.

Typical FMR spectra are shown in Fig. 3. The spectra for the parallel configuration (applied field parallel to the film plane) for all the samples show broad resonance lines, reflecting the magnetic inhomogeneity of the films. In some cases, these lines are not single Lorentzians, but the shape distortions could be interpreted as the overlap of two lines. The changes in the spectra with the angular variation of the magnetic field orientation (out-of-plane rotation) confirm that the easy axes are in the plane of the films. For samples presenting more than one resonance line, the spectra are more resolved when the applied field is closer to the film normal.

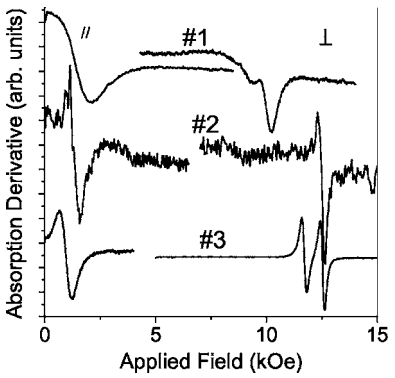

FIG. 3. FMR spectra at parallel (left) and perpendicular (right) configurations, at room temperature, and at 9.54 GHz.

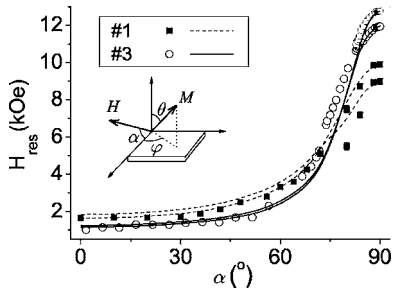

FIG. 4. Angular variation of H_{res} from the parallel to the perpendicular configuration for samples 1 and 3. The points are the experimental data and the lines simulations from Eqs. (3) and (4). g and $4\pi M_{ef}$ are the fit parameters.

For the angle dependent analysis, we have used a free energy density including the Zeeman term, the sample shape term, and an additional perpendicular effective anisotropy. Equation (1) is this free energy density in spherical coordinates. φ and θ, where θ is measured from the film normal, are the angles for the magnetization $\langle M\rangle$, and $4\pi M_{ef}$ is the effective magnetic polarization (the coordinate system is shown in Fig. 4). $4\pi M_{ef}$, shown in Eq. (2), includes all the contributions to the perpendicular anisotropy, formally separated in the shape of the film ($4\pi\langle M\rangle$) and other additional contributions (H_A).

$$f = -\langle M\rangle H(\sin\theta\cos\alpha\cos\varphi + \cos\theta\sin\alpha) + \langle M\rangle 2\pi M_{ef}\cos^2\theta. \quad (1)$$

$$4\pi M_{ef} = 4\pi\langle M\rangle + H_A. \quad (2)$$

In order to simulate the behavior of the resonance fields as a function of the angle between the applied field direction and the film plane (α, measured from the film plane), the magnetization equilibrium equations (3) and the resonance condition (4) were used.[1,2,4]

$$f_\varphi = 0 \Rightarrow \varphi_o = 0$$

$$f_\theta = 0 \Rightarrow 2H_{res}\cos(\theta_o + \alpha) = -4\pi M_{ef}\sin(2\theta_o). \quad (3)$$

$$\left(\frac{\omega}{\gamma}\right)^2 = H_{res}\cos\alpha\csc\theta_o[-4\pi M_{ef}\cos(2\theta_o) + H_{res}\sin(\theta_o + \alpha)], \quad (4)$$

where ω is the resonance frequency, γ is the magnetomechanical ratio, φ_o and θ_o are the equilibrium angles for the magnetization, and f_θ and f_φ are the first derivatives of the free energy density with respect to each angle.

Figure 4 shows that these simulations are in good agreement with the experimental data. As Eq. (3) is a transcendental equation, there is no explicit closed form solution for θ_o and we cannot simply substitute θ_o in Eq. (4). Therefore, the values of H_{res} are simulated in a recurrence way. Arbitrary values of θ_o and $4\pi M_{ef}$ are tested until they satisfy Eq. (3) for each experimental value of α and H_{res}. Next, these values are used in Eq. (4) to determine g and simulate H_{res}. The better values of g and $4\pi M_{ef}$ are the ones that provide the smaller χ^2 statistical parameter for H_{res}. g obtained in this way is also an effective parameter.

The values of g and $4\pi M_{ef}$ obtained from the simulations with Eqs. (1) and (2) are the same (considering the experimental uncertainties) as determined using the usual Kittel resonance conditions at the parallel and perpendicular configurations.[2,7]

IV. DISCUSSION

The spectra for the samples 1 and 3 show clearly two resonance lines that extend from about $\alpha=75°$ and $\alpha=82°$, respectively, until the perpendicular configuration $\alpha=90°$ (see Fig. 4). For sample 1, there are aspects of the shape of the spectra at small values of α that can be also attributed to the presence of two resonance lines.

If one considers only the region where the two lines are well resolved for samples 1 and 3, one of the lines could be associated to the main mode and the other one to a surface mode. But this interpretation did not lead to good results considering the surface inhomogeneity (SI) model.[1,2,4,5] Indeed, for these samples, the excitation of surface modes is supposed to be improbable as their thicknesses are too small. The failure of the SI model in these cases and the shape of the spectra at small α were important aspects to suggest the interpretation discussed here.

The presence of two lines for sample 3 is clear only very close to the perpendicular configuration, as quoted, and there are no distortions in the spectrum at the parallel configuration. For this sample, the observed FMR peak-to-peak linewidths (ΔH) are too narrow for such a polycrystalline and heterogeneous structure. Furthermore, as the TEM images showed percolated Co layers, it is believed that there is a strong exchange interaction in each layer and some sort of interlayer coupling, which can include exchange and dipolar (as "orange peel" coupling[10]) mechanisms. As the measured g values are (2.14 ± 0.06) and (2.22 ± 0.06) considering each line separated, the origin of these contributions can be attributed to the presence of fcc and hcp Co grains in this film.[9,11] The linewidth (ΔH) for the samples at parallel and perpendicular configurations can be seen in Table I.

The lack of hcp lines for the samples 1 and 2 can be associated with a smaller magnetic volume fraction.[9] Sample 2 shows lines as narrow as the ones of sample 3, as expected due to their similar structure, but the results allow only an uncertainty of 0.1 in the g value (2.1 ± 0.1). Similar results $(g=2.0\pm0.1)$ were obtained for sample 1, where the lines are rather broader than in the spectra of samples 2 and 3.

For the samples studied in this work, below and above the metal-insulator transition, with Co grains of few nanometers embedded in a SiO_2 matrix, one can imagine systems with at least two competing interactions, magnetic dipolar and direct exchange interaction. The dipolar interaction dominates the magnetic behavior in the insulating film, and the exchange coupling becomes more important in the metallic films. There will be a strong shape effect in the FMR measurements if any of those interactions is present in the whole film. A "mean" or "effective" interaction present in the

TABLE I. Peak-to-peak linewidth at parallel and perpendicular configurations and the predicted particle shape considering the model proposed by Dubowik. r is the ratio between the major and minor axes of the particles, f is the magnetic volume fraction, and ΔN^P is the difference between the easy and hard demagnetization factors of the particles. The acceptable mean shapes are presented in bold letters.

Sample	$\Delta H_{\parallel}$ (kOe)	$\Delta H_{\perp}$ (kOe)	F	ΔN^P	r and particle shape
1	1.7±0.2	0.52±0.07	0.28	5.5	$r\sim 2.9$, oblate, a in plane or $r\sim 6.3$, prolate, c in plane
	1.8±0.2	1.3±0.2		6.9	$r\sim 3.9$, oblate, a in plane
2	0.53±0.04	0.29±0.03	0.29	−3.6	$r\sim 2.0$, oblate, c in plane or $r\sim 2.4$, prolate, a in plane
3	0.56±0.04	0.27±0.02	0.33	−3.5	$r\sim 2.0$, oblate, c in plane or $r\sim 2.3$, prolate, a in plane
		0.26±0.02		−1.3	$r\sim 1.3$, oblate, c in plane or $r\sim 1.3$, prolate, a in plane

whole film is intrinsically assumed in the $4\pi M_{ef}$ term. As the experimental data for the samples 1, 2, and 3 could be reproduced quite well by these equations (Fig. 4), one can say that for all these samples there is an interaction reaching the whole film.

The film shape contribution ($4\pi\langle M\rangle$), obtained from the magnetization measurements, and the differences (H_A) between $4\pi M_{ef}$ and $4\pi\langle M\rangle$ are presented in Fig. 5. For sample 2, H_A corresponds to 20% of the effective perpendicular anisotropy (i.e., the effective magnetic polarization $4\pi M_{ef}$ =9050 G). Such percentage is still smaller for sample 3, showing a clear preponderance of the film shape on both resonance lines, whose origin was discussed previously. For sample 1, H_A corresponds to ~40% of $4\pi M_{ef}$; therefore, the film shape is not so preponderant and it is necessary to analyze each resonance signal more carefully. For this film, the lines are larger than the ones of samples 2 and 3. It is worth noting that in a perpendicular configuration (see Fig. 3), where the lines of sample 1 are well resolved, the lower field line is rather broader than the other.

The predicted dependence of the linewidth in the insulating FM is usually made with the "two-magnon" model, in which the main relaxation mechanism of the uniform mode involves two magnons (not necessarily with wave vectors k =0). Depending on the behavior of the magnon-magnon interaction coefficient as a function of k, such a model can lead to distinct linewidth behaviors. Being independent of k, for instance, such a coefficient leads to $\Delta H \propto H_p^2/H_{ex}^{3/2}$, where H_p is the mean square fluctuation of the effective local field and H_{ex} the exchange field, which shows directly an exchange narrowing effect.[12] But in a treatment including the k dependence in the interaction coefficient,[13] where the magnetic inhomogeneity of the local field comes mainly from the polycrystallinity, the dependence is more intricate. Under these assumptions, it is observed that the linewidths follow the local field behavior for "large," strong inhomogeneities, and the simple two-magnon model for "small," weak inhomogeneities. Large and small can be associated to the size of the magnetic particles in a granular system. For the purpose of the present discussion, a qualitative approach and some estimates will be employed, since for a precise ΔH prediction, at least the intrinsic damping parameter and the mean internal perturbation field should be known.

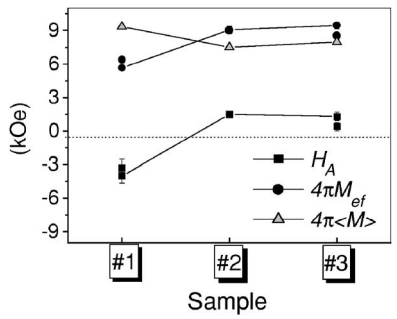

FIG. 5. Values of the magnetization from the experimental $M(H)$ curves and effective anisotropy parameters from FMR measurements for the films.

From the shape of the measured spectra for these $Co-SiO_2$ films and from the typical size of the Co grains, the small inhomogeneity regime seems to be more adequate to explain the results of sample 1. This means one should expect that $\Delta H \sim H_p^2/4\pi M_{grain}$ for $H_p \ll M_{grain}$ or $\Delta H \sim H_p$ for $H_p \gg M_{grain}$, where $Hp \sim K_{grain}/M_{grain}$, with K_{grain} being the effective uniaxial anisotropy constant of the magnetic grains. For the samples studied here, one can estimate $H_p \sim 2M_{grain}$, and those approximations imply $\Delta H \sim 2400$ Oe and $\Delta H \sim 2000$ Oe, respectively, which are values of the same order of magnitude of ΔH for the broader resonance line in the spectra of sample 1. As regards the presence of two lines, they can be interpreted assuming that this sample is composed of at least two sets of particles: a set formed by particles interacting weakly would be responsible for the broad signal, and a set formed by strongly interacting particles would be responsible for the narrow signal.[5] In the strongly interacting set of particles, the exchange interaction can be predominant, for instance, while the dipolar coupling can be the main interacting mechanism for the weakly exchange coupled set. A stronger interaction leads to smaller linewidths and also to bigger shifts in the angular variation with respect to the applied field.

Regarding the smallest values of ΔH for the metallic samples 2 and 3, they can be justified by the strong interactions in each Co layer.

In order to interpret the contributions to the effective anisotropy, the Dubowik model for shape anisotropy of magnetic heterostructures will be considered.[7] This model has been proposed to carry out all the shape effects in a combi-

nation of the sample shape contribution and the shapes of the magnetic structures (grains, layers, etc.). The magnetization of the system is assumed as $M(r)=\langle M\rangle+\delta M(r)$, restricting the spatial variation in a second term smaller than the average value expressed by the first term. From this starting point, the magnetic self-energy can be calculated and the anisotropy expressed as

$$K_{sh}=\tfrac{1}{2}\Delta N^{M}\langle M\rangle^{2}+\tfrac{1}{2}\Delta N^{P}(\langle M^{2}\rangle-\langle M\rangle^{2}), \tag{5}$$

where ΔN^{M} and ΔN^{P} are the differences between the demagnetization factors parallel and perpendicular to the easy axis of the macroscopic (sample) and microscopic (particles) demagnetization tensor, respectively. The magnetic particles are assumed to be identical. The magnetization terms are $\langle M\rangle=Mf$ and $\langle M^{2}\rangle=M^{2}f$, with the magnetic content of magnetization M in a volume fraction f. Equation (5) is the representation of the fact that there is an additional term to the anisotropy, besides the sample shape term, when dealing with a granular medium. In the FMR approach, Eq. (5) leads to the following expression for the effective magnetic polarization of the film:

$$4\pi M_{ef}=\frac{2K_{sh}}{\langle M\rangle}=4\pi\langle M\rangle+\Delta N^{P}\left(\frac{\langle M^{2}\rangle}{\langle M\rangle}-\langle M\rangle\right). \tag{6}$$

Although the dipolar interaction is not explicitly expressed in the proposed derivation of Eqs. (5) and (6), its presence is considered by using the sample demagnetizing field as $N^{M}\langle M\rangle$. In a more general way, the actual situation can be represented by

$$\begin{aligned}4\pi M_{ef}&=4\pi\langle M\rangle+H_{A}\\&=4\pi\langle M\rangle+\Delta N^{P}\left(\frac{\langle M^{2}\rangle}{\langle M\rangle}-\langle M\rangle\right)+h,\end{aligned} \tag{7}$$

where all the other possible contributions to the anisotropy, besides the ones in Eq. (6), are represented by h. H_A that was previously defined in Eq. (2) can be directly obtained from this treatment including h.

When the percentage contribution of H_A to $4\pi M_{ef}$ is significant, as happens for the samples studied in this work, one can verify the validity of the Dubowik model. Assuming that h is a small contribution, the values of ΔN^{P} have been calculated (this means that ΔN^{P} is an average representing the actual distribution of this parameter). Considering the expressions for a general ellipsoid, the possible values of the ratio between its major and minor axes ($r=c/a$) were determined, and therefore, the possible shapes of the particles could be predicted. The results can be seen in Table I, and for the majority of the lines there are two possible mean shapes. For samples 2 and 3, one of the possible shapes would be oblate particles with the c axis in plane, that are in good agreement with the TEM image of sample 3 [see Fig. 1(b)]. Then for these samples, the contribution based on the particles shape seems to be enough for justifying the FMR results and h can be disregarded. The same does not occur for sample 1, the possible shapes are not in reasonable agreement with the TEM images and h is important.

The failure of the above calculation for sample 1 can be discussed estimating h from the measured values of $4\pi M_{ef}$ and $4\pi\langle M\rangle$ and calculating the contribution from particles shape with $r\sim 1.5$ for oblate ellipsoids [as suggested by the TEM image in Fig. 1(a)]. If the c axis of the particles is assumed in the film plane, $h\approx -4000$ Oe and $h\approx -4700$ Oe for the thin and broad lines, respectively. These values are of the same order of H_A showing that, in fact, h is the main part of H_A in this sample (where H_A is of the order of 40% of the effective perpendicular anisotropy).

The origin of this additional anisotropy (h) is not clear, but its occurrence is far more significant in the insulating film than in the metallic ones. This can be related with the possible presence of two sets of particles in the film 1.

V. CONCLUSIONS

FMR results obtained with thin $Co-SiO_2$ granular films around the metal-insulator transition have been analyzed. The samples were sequentially deposited by means of dc (Co) and rf (SiO_2) sputtering, and previously characterized by TEM, magnetization, and electrical conductivity measurements. The general behavior of the applied field for resonance could be justified with a resonance condition considering effective out-of-plane anisotropies. One applied a dipolar interaction model developed for magnetic heterostructures on the interpretation of these anisotropies, which permitted an investigation of different contributions to the FMR spectra. The anisotropy terms caused by the magnetic particles shape and by the film shape can explain the results for two metallic samples in which the film shape is the preponderant contribution. But it is not sufficient to justify the results for an insulating sample, where an additional anisotropy seems to be important. The heterogeneity of the magnetic media and the magnetic particles interactions could be analyzed considering the observed FMR linewidths. In particular for the insulating sample, the FMR spectra suggest the existence of at least two sets of particles having different properties.

ACKNOWLEDGMENTS

This work was financially supported by CAPES, FAPESP, CNPq, and FAEP-UNICAMP Brazilian agencies. The samples were produced at LMMM-UFSM, Santa Maria, Brazil, in collaboration with L. S. Dorneles and L. F. Schelp. The TEM images were performed at the *Laboratório de Microscopia Eletrônica* (LME—LNLS), Campinas, Brazil.

[1]W. Wang, Z. Jiang, and Y. Du, J. Appl. Phys. **78**, 6679 (1995).
[2]J. Gómez, A. Butera, and J. A. Barnard, Phys. Rev. B **70**, 054428 (2004).
[3]S. M. Rezende, C. Chesman, M. A. Lucena, M. C. de Moura, A. Azevedo, F. M. Aguiar, and S. S. P. Parkin, J. Appl. Phys. **85**, 5892 (1999).
[4]L. J. Maksymowicz and H. Jankowski, J. Magn. Magn. Mater. **109**, 341 (1992).
[5]M. J. M. Pires, A. M. Mansanares, E. C. da Silva, J. E. Schmidt, R. Meckenstock, and J. Pelzl, J. Magn. Magn. Mater. **300**, 382 (2006).
[6]R. E. Camley, J. Magn. Magn. Mater. **200**, 583 (1999).
[7]J. Dubowik, Phys. Rev. B **54**, 1088 (1996); J. Dubowik, Phys. Rev. B **62**, 727 (2000).
[8]J. C. Denardin, M. Knobel, L. S. Dorneles, and L. F. Schelp, Mater. Sci.

Eng., B **112**, 120 (2004).
[9]L. M. Socolovsky, J. C. Denardin, A. L. Brandl, M. Knobel, and X. X. Zhang, J. Magn. Magn. Mater. **262**, 102 (2003).
[10]B. D. Schrag *et al.*, Appl. Phys. Lett. **77**, 2373 (2000).
[11]M. Farle, Rep. Prog. Phys. **61**, 755 (1998).
[12]A. M. Clogston, J. Phys. Chem. Solids **1**, 129 (1956).
[13]R. D. McMichael, D. J. Twisselmann, and A. Kunz, Phys. Rev. Lett. **90**, 227601 (2003).